




The transport properties of ultrathin 2H-NbSe₂

HPSTAR
1107-2021L B Lei^{1,2,3}, C Zhang^{2,3,4}, A B Yu^{2,3,4}, Y F Wu⁵, W Peng^{2,3,4} , H Xiao⁶ , S Qiao^{1,2,3,4} and T Hu⁵ ¹ ShanghaiTech University, Shanghai 201210, People's Republic of China² State Key Laboratory of Functional Materials for Informatics, Shanghai Institute of Microsystem and Information Technology, Chinese Academy of Sciences, Shanghai 200050, People's Republic of China³ CAS Center for Excellence in Superconducting Electronics (CENSE), Shanghai 200050, People's Republic of China⁴ University of Chinese Academy of Sciences, Beijing 100049, People's Republic of China⁵ Beijing Academy of Quantum Information Sciences, Beijing 100193, People's Republic of China⁶ Center for High Pressure Science and Technology Advanced Research, Beijing 100094, People's Republic of ChinaE-mail: hutao@baqis.ac.cn and qiaoshan@mail.sim.ac.cn

Received 10 August 2020, revised 12 November 2020

Accepted for publication 7 December 2020

Published 14 January 2021



Abstract

The competing orders arising in a two-dimensional limit are the key to understanding unconventional superconductivity. The monolayer NbSe₂ possessing a charge density wave (CDW) and superconducting orders provides a playground to study unconventional superconductivity. Here we fabricate an ultrathin 2H-NbSe₂ device based on the mechanical exfoliation method and our electrode transfer technique. Detailed four-lead and two-lead transport measurements are performed in the ultrathin sample. The superconducting transition (T_c) at 4.3 K and CDW transition at 70 K are found in the sample, consistent with the literature report for ultrathin 2H-NbSe₂. The superconducting gap (Δ) of ultrathin 2H-NbSe₂ is estimated by fitting the two-lead transport spectroscopy with the Blonder-Tinkham-Klapwijk (BTK) theory. We found that $\Delta(T)$ exhibits a BCS-like temperature dependence with $\Delta \approx 1.1$ meV at 0 K and $\Delta/k_B T_c \approx 3$. Meanwhile the gap-like features persist in the normal state and become unresolvable with the increasing temperature and magnetic field, suggesting a possible precursor superconductivity similar to the cuprate superconductors. Our results provide a new insight into superconductivity in ultrathin 2H-NbSe₂.

Keywords: superconducting gap, charge density wave, NbSe₂

(Some figures may appear in colour only in the online journal)

1. Introduction

2H-NbSe₂, belonging to the transition metal dichalcogenide family, has recently attracted a lot of interest because of the coexistence of superconductivity and charge density wave (CDW) order in this material at the two-dimensional (2D) limit [1–4]. CDW is a type of electronic ordering, exhibiting a periodic modulation of the electronic charge density [5]. The CDW phase makes the superconductivity unconventional [6–9]. The bulk 2H-NbSe₂ exhibits the incommensurate CDW order at $T_{CDW} = 33$ K and superconductivity at

$T_c = 7.2$ K [10–12]. With the increasing disorder, the T_{CDW} of 2H-NbSe₂ is found to monotonically decrease, while T_c increases, suggesting a strong correlation between the CDW and superconducting phases [13].

For an ultrathin 2H-NbSe₂, the T_c [14, 15] as well as the superconducting gap [16], decreases with lowering the sample thickness. The reduced T_c is thought to be caused by the suppression of the Cooper pair density at the superconductor–vacuum interface and the changes in the electronic band structure [16]. Along with the suppression of T_c , the superconducting gap of 2H-NbSe₂ changes from two-gap in bulk

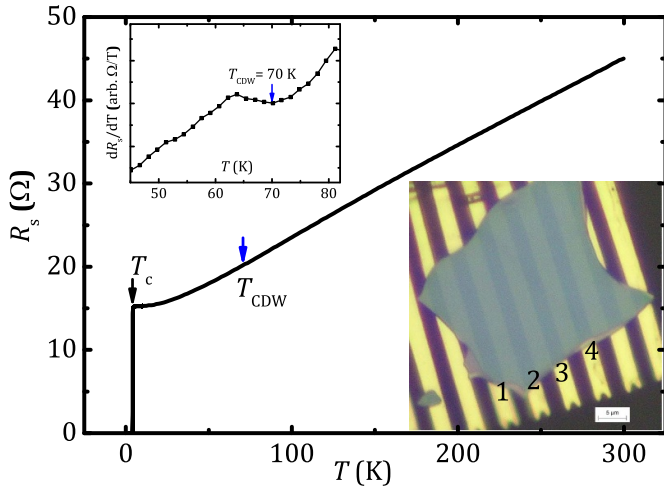


Figure 1. Temperature T dependence of the sheet resistance R_s measured at 0 T for the ultrathin 2H-NbSe₂ sample. The black and blue arrows represent the superconducting (T_c) and CDW transition temperature (T_{CDW}), respectively. Top inset: the differentiate resistance dR_s/dT vs T . The dR_s/dT shows a dip at T_{CDW} . Bottom inset: optical image of the ultrathin 2H-NbSe₂ sample. The scale bar is 5 μ m. The R_s is measured through electrodes numbered 1, 2, 3 and 4, and the two-point measurements through electrodes numbered 2 and 3.

material [17] to an anisotropic single-gap in thin-film [16]. In addition, monolayer NbSe₂ exhibits a dramatic in-plane upper critical field ($H_{c2}^{||ab}$) more than six times the Pauli paramagnetic limit, which is related to competition between the large intrinsic spin-orbit interactions (SOI) in monolayer NbSe₂ and the Zeeman effect [18]. On the other hand, the T_{CDW} increases significantly from 33 K in the bulk to 145 K in a single layer [1] and a CDW gap of $\Delta = 4$ meV at the Fermi energy [2].

In this paper, by using the mechanically exfoliation method and our electrode transfer technique, we fabricate the ultrathin 2H-NbSe₂ samples and carry out detailed transport measurements. The sample shows $T_c = 4.3$ K and $T_{CDW} = 70$ K. We found its superconducting gap is $\Delta = 1.1$ meV at 0 K and the gap features persist in the normal state, suggesting that a possible precursor superconductivity arises in ultrathin monolayer 2H-NbSe₂.

2. Experiment

The 2H-NbSe₂ device is fabricated based on the mechanical exfoliation method [19] and the developed electrode transfer technique [20]. The fabrication process is performed in a glove bag filled with argon gas. First, the bulk single-crystal 2H-NbSe₂ (commercial crystals, Prmat (Shanghai)) is cleaved into layers with scotch tape, and pressed against a Si/SiO₂ substrate. Then, the thin 2H-NbSe₂ flakes are distinguished under an optical microscope by the color. After that, the Au electrodes prefabricated on the polyvinyl alcohol (PVA) film are accurately transferred onto the top of the selected flake of 2H-NbSe₂ by using a sample transfer stage under the microscope. Alternating current (AC) resistance and current versus voltage

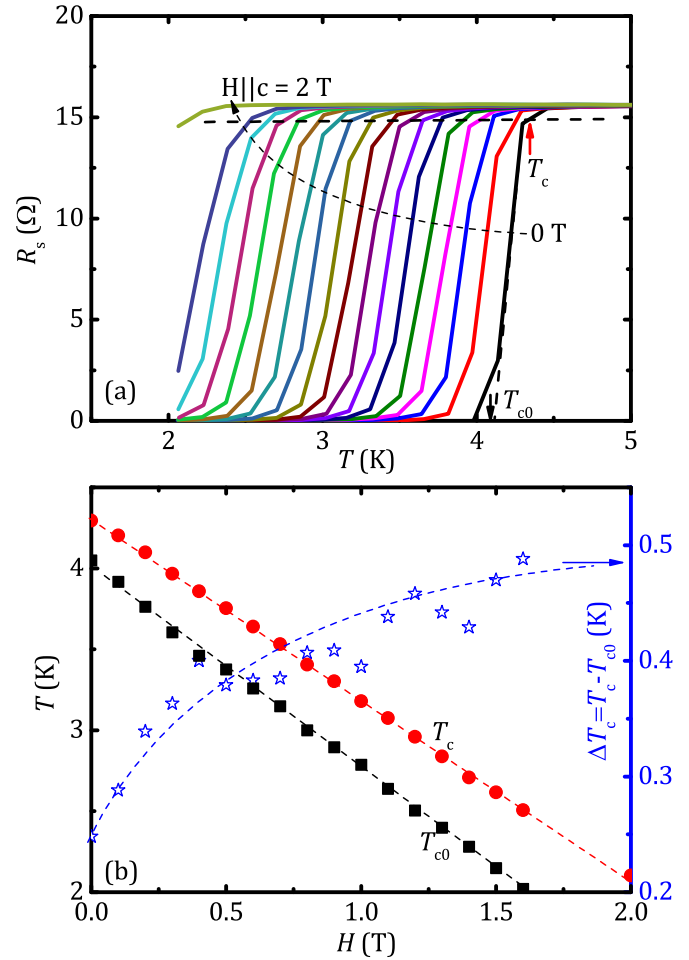


Figure 2. (a) The superconducting transition at magnetic field H ranging from 0 T to 2 T (the step is 0.1 T between 0 and 1.6 T). The T_c is defined as the temperature at which the resistance arrives at 95% of the normal state resistance as shown by the dashed line. (b) Left axis: the H - T phase diagram of the ultrathin 2H-NbSe₂ sample. The red symbols are the T_c and the black symbols are the T_{c0} . Right axis: the difference between T_c and T_{c0} .

(I - V) measurements of the 2H-NbSe₂ device are performed by using Quantum Design Electrical Transport Option (ETO).

3. Discussion

Figure 1 shows the temperature T dependence of sheet resistance (R_s) of the ultrathin 2H-NbSe₂ at zero applied field. The optical image of the ultrathin 2H-NbSe₂ device is exhibited in the bottom inset of figure 1. The R_s is measured through the electrodes numbered 1, 2, 3 and 4, and two-point measurements through the electrodes numbered 2 and 3, which show a similar oscillation and superconducting gap value as the pair of electrodes numbered 3 and 4 (data are not shown here). On cooling down, the R_s decreases with the T , showing a convex at T_{CDW} and jumping abruptly to zero at $T_c = 4.3$ K. The convex of R_s at T_{CDW} can be clarified in the top inset of figure 1, where dR_s/dT vs T exhibits a dip at $T_{CDW} = 70$ K. Such a dip in dR_s/dT was attributed to the CDW transition [1]. It is worth noting that the $T_{CDW} = 70$ K observed here is much higher

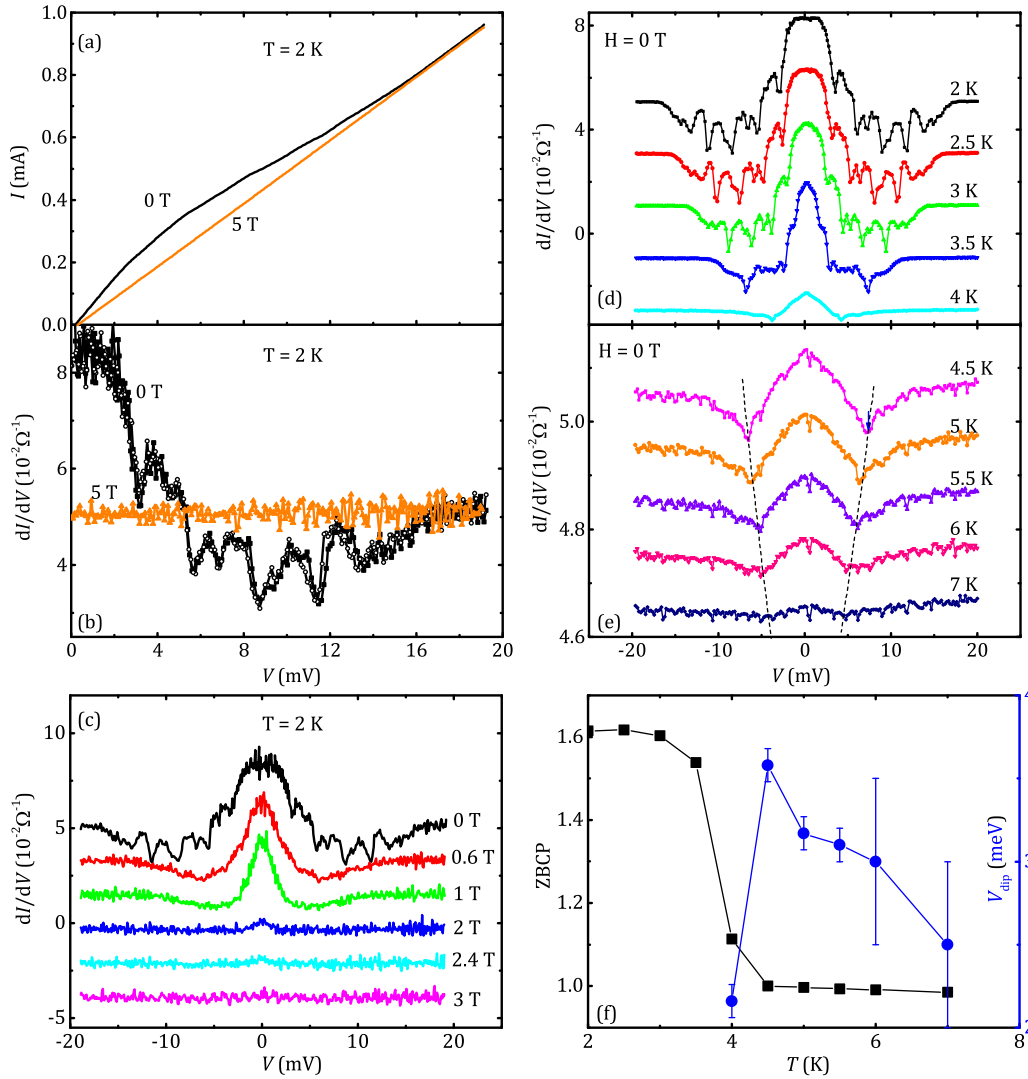


Figure 3. (a) The voltage—current (V – I) curves measured at $T = 2$ K, $H = 0$ (black curve) and 5 T (orange curve). (b) The differentiated conductance dI/dV vs V for $H = 0$ and 5 T. (c) The dI/dV measured at the applied field H ranging from 0 to 3 T. The dI/dV vs V under 0 T and below T_c (d) and above T_c (e). The curves are vertically shifted for clarity. (f) The T dependence of zero bias conductance peak (ZBCP) normalized by the normal state conductance at 4.5 K (left axis) and the voltage (V_{dip}) at the conductance dip (right axis).

than 35 K for bulk 2H–NbSe₂, consistent with the previous reports that the reduced dimension in 2H–NbSe₂ enhances the T_{CDW} . [1] Since the reduced thickness induces the opposite tendency of T_{CDW} and T_c , it thus suggests that the CDW order most likely competes with the superconducting order.

Figure 2(a) shows the $R_s(T)$ around the superconducting transition regime under various magnetic fields H from 0 to 2 T. The magnetic field H is applied in the c direction of crystalline. The T_c (red arrow in figure 2(a)) is defined as the temperature where the resistance arrives at the value of 95% normal state resistance as shown by the dashed line. The T_{c0} is the zero resistance transition temperature as indicated by the black arrow. The left axis of figure 2(b) is the H dependence of T_c and T_{c0} obtained from figure 2(a). The difference between T_c and T_{c0} is shown in the right axis of 2(b), which increases with the applied field, suggesting that the superconducting transition is broadened by the applied field.

For the sake of investigating the superconducting gap, two-point measurements are performed on the sample and the results are displayed in figure 3. Figure 3(a) shows the current–voltage (V – I) curve measured at temperature $T = 2$ K with applied field $H = 0$ and 5 T. It is found that the V shows a non-linear behavior with I at zero field, and a linear behavior at 5 T. The non-linear V – I can be understood in terms of Andreev reflection [21] from the proximity effect of the superconductor/Au electrode junction. The linear V – I reflects the ohmic behavior of the normal state. To clarify, one can differentiate the V – I curve to obtain differentiated conductance dI/dV as plotted in figure 3(b). The dI/dV at 0 T shows the peak around the zero bias voltage and several dips at the higher voltage. Actually, a maximum in dI/dV close to zero bias was previously observed in point-contact measurements with a metallic/superconducting point contact [23]. Such a behavior can be understood as a consequence of Andreev reflection (AR). AR occurs at the interface between the normal metal and the

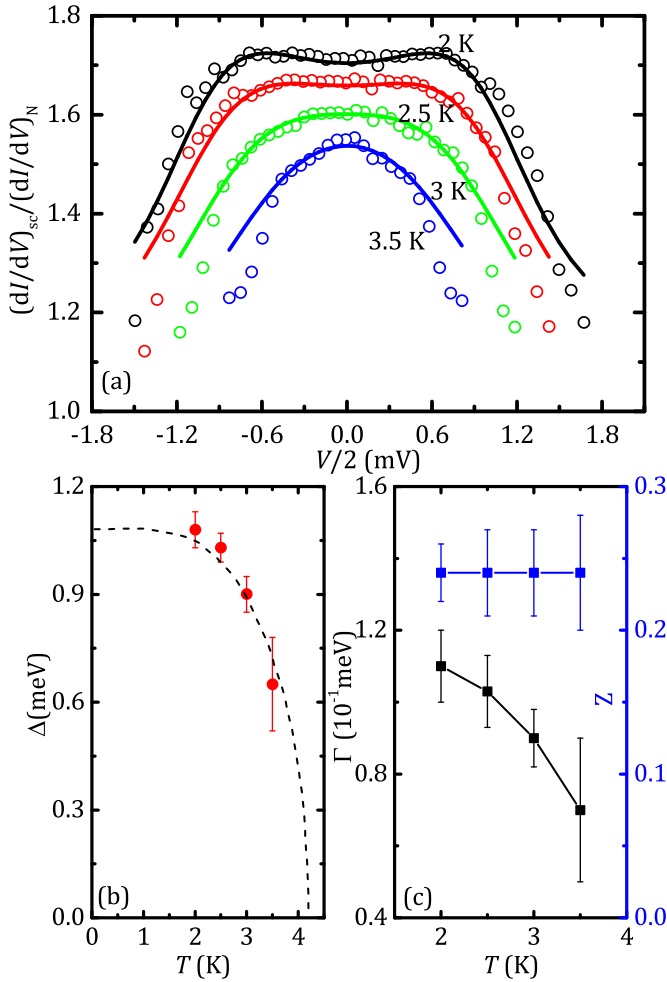


Figure 4. (a) The differential conductances (hollow symbols) at $T = 2\text{--}3.5$ K and the fitting curves (solid lines) by BTK formula. (b) T dependence of superconducting gap Δ . (c) The temperature dependence of fitting parameter Γ (left axis) and Z (right axis). Error bars are given by the uncertainty of fitting.

superconductor, where an incident electron with energy less than the superconducting energy gap (Δ) can be reflected back as a hole along a path of the incident electron (retro-reflection). Thus, AR enhances subgap conductance and leads to the maximum or peak in dI/dV . On the other hand, AR is absent in the insulator/superconductor interface, e.g. h-BN/NbSe₂ structure [16], which results in a dip in dI/dV at zero bias. Interestingly, in a graphene/superconductor structure, like graphene/NbSe₂, the retro and specular AR are expected to occur at Fermi energy (E_F) $\gg \Delta$ and $E_F \ll \Delta$, respectively [22]. By tuning E_F of graphene through applying a gate voltage, the dI/dV at zero bias is found to vary from the dip to the peak, which corresponds to a change from specular and retro AR [22]. In addition, a possible explanation for these conductance dips at higher voltage is that the contact is not in the ballistic limit at which the V_{dip} should decrease with the increase of temperature and magnetic field [23]. In our sample, the contact area between gold and NbSe₂ is on a micrometer scale, where both ballistic and non-ballistic limit contacts are expected to contribute to the conductance in parallel. Thus, the V_{dip} most

likely results from non-ballistic limit contact of electrodes with a superconductor. On the other hand, the dI/dV at 5 T remains unchanged with the increasing V suggesting a good ohmic contact between Au electrodes and 2H-NbSe₂.

Figure 3(c) shows the dI/dV vs V behavior in the various magnetic fields. At 0 T, the dI/dV shows a peak around the zero bias voltage and several dips at large V . It decreases with the increase of H and finally becomes unresolvable above 2.4 T. The large dI/dV peak below T_c is attributed to Andreev reflection with a high transparency of interfaces [21], which will be shown in figure 4. In order to get more accurate data of dI/dV , we apply a direct current (DC) and alternating current (AC) 0.01 mA on the samples. The obtained differential resistances dI/dV under different DC voltage bias are shown in figure 3(d). It is found that both the conductance peak and dip are suppressed as the temperature increases, while the feature of the gap (marked by the arrows at V_{dip} in the conductance dip) persists in the normal state up to 7 K as shown in figure 3(e). The gap behavior was also found above T_c in other two-dimensional (2D) superconductors, like the thin film of NbN [24] and LaAlO₃-SrTiO₃ interface, [25] owing to Cooper-pair localization driven by the disorder. [26] In contrast to the low-disorder NbSe₂ van der Waals heterostructure where there are no signs of persistence of gap-like features above T_c , [16, 22] our sample taking the polymers as protective encapsulating layers can induce substitutional defects and impurities [27], which may lead to a strong disorder and localized Cooper-pairs above T_c . Thus the gap-like feature above T_c in figure 3(e) reflects the possible precursor superconductivity in the normal state. In addition, the possible precursor superconductivity might not be related to the CDW order, since we do not find the gap-like feature present above $T_c = 7$ K at the bulk NbSe₂ (data are not shown here), where the CDW order still survives. The zero biased conductance peaks are summarized in figure 3(f). The left axis of figure 3(f) shows the zero bias conductance peak (ZBCP) which is normalized at the value at 4.5 K. It is found that the ZBCP decreases abruptly at around $T_c = 4.3$ K from 1.6 to around 1, suggesting the disappearance of Andreev reflection. On the other hand, the gap-like feature characterized by the V_{dip} still survives above T_c as shown in the right axis of figure 3(f).

Figure 4(a) shows the normalized differential conductances (hollow symbols) $(dI/dV)_{SC}/(dI/dV)_N$ versus $V/2$ for ultrathin 2H-NbSe₂ at 0 T and the $T = 2\text{--}3.5$ K, where $(dI/dV)_N$ is the differential conductance at 4.5 K. It is worth noting that the voltage on the junction of Au electrodes and 2H-NbSe₂ is roughly one half of the applied voltage V between two Au electrodes. Thus, we fit the data using the BTK model in one anisotropic gap [28], which relates the normalized differential conductances to superconducting gap values Δ , broadening parameter Γ and barrier parameters Z , and display the fitting curves as the solid lines shown in figure 4(a). Almost constant $Z = 0.24$ is used for fitting conductance curves. Note that Z describes the transparency of the interface and a value of Z much less than 1 suggests a high transparency barrier. The temperature dependence of broadening parameter Γ and gap Δ are also shown in figure 4(b) and the left axis of figure 4(c). The gap Δ exhibits BCS-like

behavior with $\Delta(T=0\text{K})=1.1$ meV. Here, the error bars are defined as the uncertainty due to the fit. We compare the data fitted with anisotropic and isotropic gap formula, and find there are no differences between them. The value of 1.1 meV obtained here is consistent with the literature report where $\Delta(T=0\text{K})=1.3$ meV for bulk 2H-NbSe₂ is reduced to 0.96 meV for three-layer 2H-NbSe₂. [16] Note that the $\Delta(T=0\text{K})=1.1$ meV and $T_{CDW}=70$ K in our ultrathin 2H-NbSe₂ suggest the number of NbSe₂ layers is around five, while the $T_c=4.3$ K would correspond to one or two layers. These discrepancies are most likely due to the sample quality of our ultrathin 2H-NbSe₂ being not so good owing to the use of polymers as protective encapsulating layers in this work, which can lead to doping and damaging at the interface [27] and suppress the T_c .

4. Conclusion

In summary, detailed electrical transport measurements are carried out on the ultrathin 2H-NbSe₂ single crystal. The $T_c=4.3$ K and $T_{CDW}=70$ K in the ultrathin sample. A good contact interface is found between Au electrodes and ultrathin 2H-NbSe₂. A BCS-like gap with $\Delta=1.1$ meV at 0 K is revealed in this sample. The gap-like feature is found to persist in the normal state up to 7 K. Our results suggest that possible precursor superconductivity arises in ultrathin 2H-NbSe₂.


Acknowledgments

The authors acknowledge the support of NSCF Grant No. 11574338, NSAF Grant No. U1530402 and CAS State Key Laboratory of Functional Materials for Informatics.

ORCID iDs

W Peng  <https://orcid.org/0000-0002-9888-1891>

H Xiao  <https://orcid.org/0000-0001-8859-9967>

T Hu  <https://orcid.org/0000-0003-0338-9632>

References

- [1] Xi X, Zhao L, Wang Z, Berger H, Forró L, Shan J and Mak K F 2015 *Nat. Nanotechnol.* **10** 765–9
- [2] Ugeda M M *et al* 2016 *Nat. Phys.* **12** 92–7
- [3] Wang H *et al* 2017 *Nat. Commun.* **8** 1–8
- [4] Xing Y *et al* 2017 *Nano Lett.* **17** 6802–7
- [5] Grüner G 1988 *Rev. Mod. Phys.* **60** 1129
- [6] Chang J *et al* 2012 *Nat. Phys.* **8** 871–6
- [7] Achkar A *et al* 2012 *Phys. Rev. Lett.* **109** 167001
- [8] Comin R *et al* 2014 *Science* **343** 390–2
- [9] da Silva Neto E H *et al* 2014 *Science* **343** 393–6
- [10] Wilson J A, Di Salvo F and Mahajan S 1975 *Adv. Phys.* **24** 117–201
- [11] Moncton D, Axe J and DiSalvo F 1975 *Phys. Rev. Lett.* **34** 734
- [12] Berthier C, Molinié P and Jérôme D 1976 *Solid State Commun.* **18** 1393–5
- [13] Cho K *et al* 2018 *Nat. Commun.* **9** 1–9
- [14] Staley N E, Wu J, Eklund P, Liu Y, Li L and Xu Z 2009 *Phys. Rev. B* **80** 184505
- [15] Cao Y *et al* 2015 *Nano Lett.* **15** 4914–21
- [16] Khestanova E *et al* 2018 *Nano Lett.* **18** 2623–9
- [17] Noat Y *et al* 2015 *Phys. Rev. B* **92** 134510
- [18] Xi X, Wang Z, Zhao W, Park J H, Law K T, Berger H, Forró L, Shan J and Mak K F 2016 *Nat. Phys.* **12** 139–43
- [19] Geim A K and Novoselov K S 2010 *The rise of graphene Nanoscience and Technology: A Collection of Reviews From Nature Journals* (Singapore: World Scientific) pp 11–19
- [20] Zhang C, Hu T, Wang T, Wu Y, Yu A, Chu J, Zhang H, Xiao H, Peng W, Di Z *et al* 2020 (arXiv: 2006.03338 [cond-mat.supr-con])
- [21] Andreev A 1964 *Sov. Phys. JETP* **19** 1228
- [22] Efetov D K *et al* 2016 *Nat. Phys.* **12** 328–32
- [23] Sheet G, Mukhopadhyay S and Raychaudhuri P 2004 *Phys. Rev. B* **69** 134507
- [24] Sacepe B, Chapelier C, Baturina T I, Vinokur V M, Baklanov M R and Sanquer M 2010 *Nat. Commun.* **1** 1–6
- [25] Richter C *et al* 2013 *Nature* **502** 528–31
- [26] Sacépé B, Dubouchet T, Chapelier C, Sanquer M, Ovdia M, Shahar D, Feigel’Man M and Ioffe L 2011 *Nat. Phys.* **7** 239–44
- [27] Jung Y *et al* 2019 *Nat. Electron.* **2** 187–94
- [28] Hayashi N, Ichioka M and Machida K 1996 *Phys. Rev. Lett.* **77** 4074